JOURNAL OF GEOPHYSICAL RESEARCH, VOL. 87, NO. B11, PAGES 9247-9257, NOVEMBER 10, 1982

An Assessment of ^{40}Ar-^{39}Ar Dating of Incompletely Degassed Xenoliths

A. R. GILLESPIE,[1] J. C. HUNEKE, AND G. J. WASSERBURG

Lunatic Asylum, Division of Geological and Planetary Sciences, California Institute of Technology Pasadena, California 91125

The possibility of measuring the age of eruption of Pleistocene lavas by ^{40}Ar-^{39}Ar analysis of entrapped ancient potassic xenoliths is demonstrated by a study of model systems. Upon inclusion in the hot magma such xenoliths are commonly only partially degassed of radiogenic ^{40}Ar which has accumulated in them since their original crystallization. The residual ^{40}Ar will increase the apparent K/Ar age of the xenolith. However, if a xenolith is of Cretaceous age or younger, then a plateau in its ^{40}Ar-^{39}Ar age spectrum giving the age of eruption is expected to extend over 25–50% of the total ^{39}Ar released if degassing of the xenolith in the magma exceeded 90% and if the phases in the xenolith are characterized by sufficiently different diffusion dimensions or activation energies. If diffusion was from a bimodal population of spheres, then the radii must differ by a factor of 10 or more (or the diffusion coefficients by a factor of 100 or more); or if the spheres were equal in size (and in diffusion coefficients), then the activation energies must differ by a factor of at least 1.5. That such requirements may be realized in real xenoliths containing K-feldspars is expected from published activation energies for microcline and from data determined on a granitic xenolith which was degassed in an early Pleistocene basalt flow. The experimental results appear to establish that old xenoliths may contain Ar in distinctive phases which degas at sufficiently different temperatures as to permit determination of the age of degassing or eruption.

1. INTRODUCTION

To establish a chronological framework for late Quaternary events, it is frequently necessary to obtain precise age information on volcanic basalt eruptions which have well-defined stratigraphic relationships. However, few reliable absolute dating techniques are available for such young samples. *Radicati di Brozolo et al.* [1981] demonstrated that accurate ages could be obtained on leucites from volcanic tuffs 0.35 m.y. in age by the ^{40}Ar-^{39}Ar variant of K/Ar dating and by high precision Rb-Sr measurements. The success of these experiments was due primarily to the availability of coarse-grained material with a high K content for the application for the ^{40}Ar-^{39}Ar technique. While most basic lavas do not have the required potassic phenocrysts, K-rich xenoliths of older granitic rocks incorporated in the magma during eruption may satisfy this requirement. They would be attractive for K/Ar dating if they had lost their radiogenic ^{40}Ar during heating in the magma. *Hart* [1964] showed that such degassing did occur in wall rock near an intruded stock. *Dalrymple* [1964] considered the possibility of dating a basalt by analyzing degassed granitic xenoliths, but he found anomalously high conventional K/Ar ages. This he attributed to incomplete degassing of ^{40}Ar from the xenoliths during heating in the magma. However, in principle, the dating of such xenoliths by stepwise thermal release of ^{40}Ar and ^{39}Ar could reveal the time of degassing of the less retentive sites in the xenolith and thus the age of eruption of the host basalt.

We assess here those factors which determine whether or not an eruption age can indeed be determined through the study of incorporated xenoliths. It must be demonstrated both that there are reasonable conditions under which a reservoir of ^{40}Ar in the xenolith may be sufficiently degassed during eruption to yield at a later date an age plateau corresponding to the time of eruption and that during the analysis of the Ar released during the laboratory heating steps, the ^{40}Ar contributed from other incompletely degassed reservoirs is not so large as to mask this plateau. The model we explore may be readily generalized and can include the assessment of formation as well as eruption age plateaus. Finally, we present the results of a ^{40}Ar-^{39}Ar analysis of a granitic xenolith from an early Pleistocene basalt flow in the Sierra Nevada, California, to compare the behavior of a partially degassed rock with the theoretical models. *Berger* [1975] has already shown that it may be possible to estimate the ages of Tertiary or older thermal events by ^{40}Ar-^{39}Ar analysis of 1400-m.y.-old material intruded 60 m.y. ago.

2. DEVELOPMENT OF ERUPTION AGE PLATEAUS

To assess the feasibility of obtaining reasonable eruption ages from partially degassed xenoliths, we have described by simple volume diffusion the Ar loss from spheres in a model xenolith during heating in a magma and subsequent heating in the laboratory for ^{40}Ar-^{39}Ar analysis, assuming different grain size distributions and activation energy distributions for the groups of spheres composing the model xenolith. The diffusion characteristics of the material of each sphere are assumed to be uniform and isotropic. Diffusion out of the grains is described by Fick's law, which for radial diffusion in isotropic spheres is

$$\frac{\partial C(r, t)}{\partial t} = D[T(t)] \frac{1}{r^2} \frac{\partial}{\partial r} \left[r^2 \frac{\partial C(r, t)}{\partial r} \right] \quad (1)$$

where $C(r, t)$ is the concentration of Ar, r is radial distance from the center of the sphere, t is time, and D is the diffusion coefficient. The concentration of Ar at the sphere boundaries ($r = a$) is taken to be zero and the concentration of ^{40}Ar and K is uniform for all grains at $t = 0$, the time the xenolith is engulfed by the magma. The original ^{40}Ar abundance is taken to correspond to an age t_0. The diffusion coefficient is

[1] Now at Jet Propulsion Laboratory, Pasadena, California 91109.

Paper number 2B1138.
0148-0227/82/002B-1138$05.00

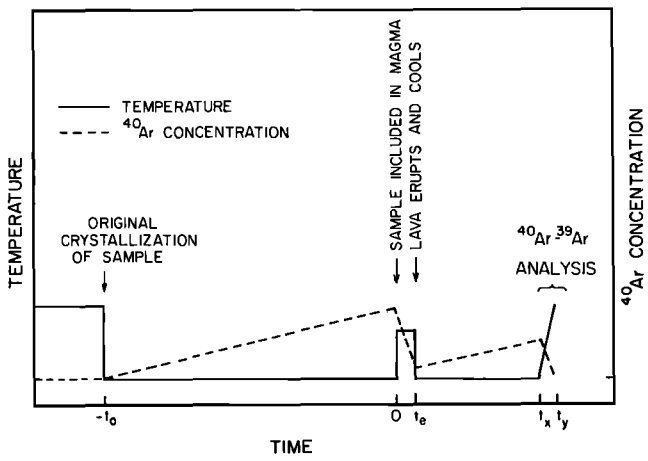

Fig. 1. Schematic history of temperature and ^{40}Ar accumulation in a model xenolith. From $t = -t_0$, the time of original crystallization, to $t = 0$, ^{40}Ar accumulates without loss. The ^{40}Ar is lost from the model xenolith during heating in the magma from $t = 0$ to $t = t_e$; and after cooling, ^{40}Ar once again accumulates until t_x and is added to the residue which was not degasssed from $t = 0$ to $t = t_e$. All ^{40}Ar is extracted during analysis from t_x to t_y. For simplicity, t_e and t_y-t_x are considered to be much shorter time intervals than t_0 or t_x-t_e, and ^{40}Ar accumulated during these short intervals is ignored.

related to the temperature $T(t)$ by the Arrhenius relation

$$D[T(t)] = D_0 \exp[-Q/RT(t)] \tag{2}$$

where R is the gas constant, Q the activation energy for diffusion, and D_0 a characteristic constant. Figure 1 illustrates the temperature history imposed on the model xenoliths. Diffusive loss of Ar begins at $t = 0$, as the grains are heated in the magma. The temperature of the xenolith and thus the diffusion coefficient varies with time t after the xenolith was incorporated in the magma at $t = 0$, and this variation in D is accounted for by introducing the dimensionless variable

$$\tau \equiv (D_0/a^2) \int_0^t \exp[-Q/RT(\eta)]\, d\eta \tag{3}$$

where a is the grain radius. Shortly after eruption, the lava freezes and the xenolith cools sufficiently to stop diffusion at $t = t_e$. Thus a fraction $F(\tau_e)$ of the ^{40}Ar present in a grain at $t = 0$ is lost by t_e, where $\tau_e = \tau\{D[T(t)], t_e, a\}$. We assume that there is no further loss of Ar from t_e to t_x, when analysis is begun, and that $t_e/t_0 \ll 1$. After t_e, radiogenic ^{40}Ar again begins accumulating from the decay of ^{40}K, and this is added to the residue of the original radiogenic ^{40}Ar which was not degassed during heating in the magma. We denote the concentration of new ^{40}Ar formed after t_e by $C_N{}^{40}$. After the sample is brought to the laboratory at time t_x, it is neutron irradiated to produce ^{39}Ar via $^{39}K(n, p)^{39}Ar$ reactions. Thus at t_x there is (1) the new (N) ^{40}Ar created since t_e, (2) the residue of original (O) ^{40}Ar created before $t = 0$, and (3) ^{39}Ar. The number and concentration (per unit volume) of atoms of each kind of Ar in the sphere are denoted by $N_N{}^{40}$, $N_O{}^{40}$, N^{39}, and $C_N{}^{40}$, $C_O{}^{40}$, and C^{39}, respectively. For the case where the diffusion coefficient is a function of time, we may change the 'time' variable to τ as given in (3) and obtain the cumulative fraction F of Ar lost from a single spherical grain [cf. *Crank*, 1956; *Carslaw and Jaeger*, 1959]. Note that τ is dependent on the species of sphere 'i' to which Q, D_0, and a pertain. The cumulative fraction of Ar lost for a given grain as a function of the integrated diffusion history is given by

$$F = 1 - \frac{6}{\pi^2} \sum_{n=1}^{\infty} \frac{1}{n^2} \exp(-\pi^2 n^2 \tau) \tag{4}$$

For reference, (4) is shown graphically in Figure 2.

A given rock sample may be considered to be made up of a distribution of grains with different values of the parameters Q_i, D_{0i}, and $a_i{}^2$, and also with different concentrations of K. For simplicity we will take the K concentration to be identical for all grains. We may express the cumulative fraction of ^{40}Ar lost by time t from a population p of m types of grains initially ($t = 0$) of uniform concentration by

$$F_p{}^{40}(t) = \sum_{i=1}^{m} a_i{}^3 M_i F(\tau_i) \Big/ \sum_{j=1}^{m} a_j{}^3 M_j \tag{5}$$

Here M_i is the number of grains of type 'i' in a unit volume, and τ_i is the value of $\tau(D_{0i}, Q_i, T(t), t, a_i)$ at time t for grains of type 'i.'

In an ^{40}Ar-^{39}Ar analysis the different Ar atoms in a sample are extracted and measured. The sample, which has already undergone Ar loss in nature, is reheated in the laboratory (L) beginning at time t_x, and diffusive loss is renewed. The temperature is increased until the sample melts at t_y, where $(t_y - t_x)/t_x \ll 1$. At any time t_L during the extraction we define the laboratory diffusion parameter $\tau_{Li} \equiv (D_{0i}/a_i{}^2) \int_{t_x}^{t_L} \exp[-Q_i/RT(\eta)]\, d\eta$ for a single type of sphere. For this sphere the fraction of the new ^{40}Ar extracted from t_x to t_L is given by $F(\tau_{Li})$. At the same time, the residual ^{40}Ar left in each sphere upon cooling at t_e is also extracted. The fraction of original ^{40}Ar extracted in the laboratory from a given sphere in the time t_x to t_L is given by $[F(\tau_{ei} + \tau_{Li}) - F(\tau_{ei})]$. This residue of original ^{40}Ar is extracted at a different rate than the new ^{40}Ar created since t_e. The total ^{40}Ar released from a sphere of type i between the times t_x and t_L is simply

$$\Delta N_i{}^{40} = \tfrac{4}{3} \pi a_i{}^3 [C_O{}^{40} \{F(\tau_{ei} + \tau_{Li}) - F(\tau_{ei})\} + C_N{}^{40} F(\tau_{Li})] \tag{6}$$

and the total rate of extraction at t_L is

$$\frac{dN_i{}^{40}}{dt_L} = \tfrac{4}{3} \pi a_i{}^3 \left[C_O{}^{40} \frac{\partial F(\tau_{ei} + \tau_{Li})}{\partial \tau_{Li}} + C_N{}^{40} \frac{\partial F(\tau_{Li})}{\partial \tau_{Li}} \right] \frac{d\tau_{Li}}{dt_L} \tag{7}$$

The ^{39}Ar created from neutron irradiation of the ^{39}K is degassed at the rate

$$\frac{dN_i{}^{39}}{dt_L} = \tfrac{4}{3} \pi a_i{}^3 C^{39} \frac{\partial F(\tau_{Li})}{\partial \tau_{Li}} \frac{d\tau_{Li}}{dt_L} \tag{8}$$

We assume that ^{39}Ar and ^{40}Ar have the same diffusion constants in each type of sphere. At any instant during the laboratory analysis, the relative rate of degassing of ^{40}Ar from the entire xenolith (p) is found from (7) to be

$$\frac{dN_p{}^{40}}{dt_L} = \sum_{i=1}^{m} \tfrac{4}{3} \pi a_i{}^3 M_i \left[C_O{}^{40} \frac{\partial F(\tau_{ei} + \tau_{Li})}{\partial \tau_{Li}} + C_N{}^{40} \frac{\partial F(\tau_{Li})}{\partial \tau_{Li}} \right] \frac{d\tau_{Li}}{dt_L} \tag{9}$$

For ^{39}Ar we have

$$\frac{dN_p^{39}}{dt_L} = C^{39} \sum_{i=1}^{m} \tfrac{4}{3}\pi a_i^3 M_i \frac{\partial F(\tau_{Li})}{\partial \tau_{Li}} \frac{d\tau_{Li}}{dt_L} \qquad (10)$$

The instantaneous ratio of ^{40}Ar/^{39}Ar released in the time interval dt_L is given by

$$\frac{dN_p^{40}}{dN_p^{39}} = \frac{C_N^{40}}{C^{39}} + \frac{C_O^{40}}{C^{39}} \left\{ \sum_{i=1}^{m} \left[a_i^3 M_i \frac{\partial F(\tau_{ei} + \tau_{Li})}{\partial \tau_{Li}} \frac{d\tau_{Li}}{dt_L} \right] \div \sum_{j=1}^{m} \left[a_j^3 M_j \frac{\partial F(\tau_{Lj})}{\partial \tau_{Lj}} \frac{d\tau_{Lj}}{dt_L} \right] \right\} \qquad (11a)$$

$$\frac{dN_p^{40}}{dN_p^{39}} = \frac{C_N^{40}}{C^{39}} + \frac{C_O^{40}}{C^{39}} Z \qquad (11b)$$

where the function Z is given by

$$Z \equiv \sum_{i=1}^{m} \left[a_i^3 M_i \frac{\partial F(\tau_{ei} + \tau_{Li})}{\partial \tau_{Li}} \frac{d\tau_{Li}}{dt_L} \right] \div \sum_{j=1}^{m} \left[a_j^3 M_j \frac{\partial F(\tau_{Lj})}{\partial \tau_{Lj}} \frac{d\tau_{Lj}}{dt_L} \right] \qquad (11c)$$

From dN_p^{40}/dN_p^{39} an apparent age A for each differential amount of Ar released is given by

$$A(t_L) = \lambda^{-1} \ln \left(1 + B \frac{dN_p^{40}}{dN_p^{39}} \right) \qquad (12)$$

where λ is the decay constant for ^{40}K and B is the scaling factor for the neutron-irradiated sample used to calculate the age. The cumulative fraction of ^{39}Ar extracted for the xenolith is given by

$$F_p^{39}(t_L) = \left(\sum_{i=1}^{m} a_i^3 M_i F(\tau_{Li}) \right) \Big/ \sum_{j=1}^{m} a_j^3 M_j$$

A plot of $A(t_L)$ versus the cumulative fraction $F_p^{39}(t_L)$ of ^{39}Ar extracted from the sample provides an exact age spectrum resulting from continuous measurement of Ar during ^{40}Ar-^{39}Ar analysis.

Writing the apparent age (equation (12)) in the form $A(t_L) = t_x + \Delta A(t_L)$, we determine the fractional increase in the apparent age over the eruption age, due to contributions from the residual original ^{40}Ar, to be

$$\frac{\Delta A(t_L)}{t_x} \approx \frac{1}{\lambda t_x} \ln [1 + (e^{\lambda t_0} - 1)Z] \approx \frac{t_0}{t_x} Z \qquad (13)$$

for the problems of interest ($\lambda t_0 \ll 1$). $\Delta A/t_x$ increases monotonically during extraction, and unless $F_p^{40}(t_e) = 1.0$, no finite fraction of argon will be extracted completely free of residual original ^{40}Ar. Therefore any plateau will yield, sensu stricto, only an upper limit to the age of eruption, but in practice, this limit may be much closer to the actual age than the precision of the argon measurements. Thus, if the xenolith is to yield a plateau at the age of eruption, $\Delta A/t_x$ must not exceed some limit ε for a significant fraction of ^{39}Ar released. This gives

$$Z \leq \varepsilon t_x/t_0 \qquad (14)$$

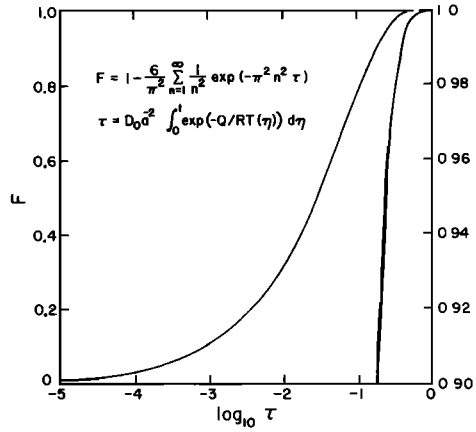

Fig. 2. Fractional loss of Ar from a spherical grain as a function of time according to the exact solution of equation (4) [cf. *Carslaw and Jäger*, 1959]. To the right of the break in the abscissa the ordinate scale has been expanded.

If the age plateau is required to encompass some fraction f of the total ^{39}Ar at the time $t_L = t_\varepsilon$ when $\Delta A/t_x = \varepsilon$ is obtained, we then have

$$f = F_p^{39}(t_\varepsilon) = \left\{ \sum_{i=1}^{m} a_i^3 M_i F[\tau_{Li}(t_\varepsilon)] \right\} \Big/ \sum_{j=1}^{m} a_j^3 M_j \qquad (15)$$

Equations (14) and (15) determine whether a basalt erupted t_x years ago may be satisfactorily dated by the ^{40}Ar-^{39}Ar analysis of an incorporated xenolith crystallized ($t_0 + t_x$) years ago. The conditions which must be specified a priori are the fractional limit ε, below which the measured age is not significantly different from the eruption age, and the extent f of the ^{39}Ar release required to define adequately an age plateau. As seen from (14), the dating experiment can succeed if t_x/t_0 is sufficiently small and/or degassing in the magma $[F_p^{40}(t_e)]$ is sufficiently great. It is clear that the larger the portion of easily degassed grains, the more easily these conditions are satisfied. A comparable formalism may be developed to establish the conditions under which a formation-age plateau may be obtained, and the two sets of criteria can be simultaneously applied to the model xenolith.

We consider first the application of these criteria to the model xenolith consisting of identical spheres. *Turner* [1968] has calculated age spectra for spheres degassed different amounts $F(\tau_e)$ immediately before analysis ($t_x = t_e$), so that $C_N^{40} = 0$. These spectra show that $F(\tau_e)$ must be large before a reasonable fraction of ^{39}Ar is released with little accompanying residual ^{40}Ar. For example, if $F(\tau_e) = 0.95$, dN_O^{40}/dN^{39} is nearly 0.01 when only 10% of the ^{39}Ar has been degassed. $F(\tau_e)$ must exceed 0.99 before a sizable fraction (e.g., 25%) of the ^{39}Ar is released unaccompanied by significant amounts of residual ^{40}Ar. This must occur if a plateau in the age spectrum identifying the age of eruption is to be developed. For instance, let us take $t_x/t_0 = 0.01$ and $C_O^{40}/C^{39} = 1$ and require that dN_O^{40}/dN^{39} be less than 5×10^{-4} when $F^{39}(\tau_L) = 0.25$ for a plateau to be considered present. To achieve this, $F(\tau_e)$ must exceed 0.999, or τ must exceed 0.651. In the discussion below, the critical value of τ_e that is necessary to achieve a plateau will be referred to as τ_{crit}.

The condition $\tau_e = \tau_{crit}$ may be achieved by heating any grain for a long enough time. This time is less if the activation energy is lower, if the radius is smaller, if D_0 is

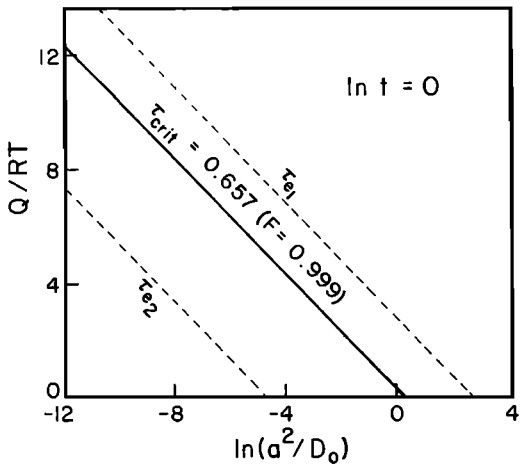

Fig. 3. The extent of degassing of a spherical grain at constant temperature is a function of the activation energy Q, the grain radius a, the value of D_0, and the time t since heating commenced. This level of degassing is specified by $\ln \tau - \ln t_e = -[Q/RT_e + \ln (a^2/D_0)]$. The figure depicts at time $t = 1$ s the distribution of all spheres degassed to $\tau = \tau_{crit}$, the level required to yield a plateau of $f = 0.25$ and $dN_O^{40}/dN^{39} < 5 \times 10^{-4}$ upon later analysis at t_x, where $t_x/t_0 = 0.01$. The effect on τ of increasing Q/RT by α is the same as decreasing D_0 by a factor of e^{α} or of increasing a by a factor of $e^{\alpha/2}$. If a population consists of two types of grains, we anticipate that a plateau at t_x may still be developed, even if the extent of degassing in the magma $[F_p^{40}(t_e)]$ is less than $F^{40}(\tau_{crit})$ for the population of identical spheres. In this case, one type of spheres will be degassed less than $F^{40}(\tau_{crit})$ and the other will be degassed in excess of $F^{40}(\tau_{crit})$, so that $\tau_{e_1} < \tau_{crit}$ and $\tau_{e_2} > \tau_{crit}$.

larger, or if the lava temperature (T_e) is higher. T_e and t_e are extrinsic to the grain, and in a given lava where t_e is the same for all grains, grains which achieve τ_{crit} have parameters specified by $-[\ln (a^2/D_0) + Q/RT_e] = \ln \tau_{crit} - \ln t_e$. This relation is shown graphically in Figure 3. Different types of spheres having values of a^2/D_0 and Q such that they plot on the line τ_{crit} at time t_e with temperature T_e will each be degassed sufficiently to yield age plateaus identifying t_x. Spheres plotting above this line will be insufficiently degassed to yield a plateau; spheres plotting below this line will be excessively degassed and will yield plateaus of greater extent.

Turner [1968] noted that while single spheres were unlikely to be degassed sufficiently to yield plateaus giving the age of reheating events, populations of spheres having different characteristics might give plateaus, even though the net level of degassing was unchanged. This can occur when a substantial fraction of the total volume of the population consists of poorly retentive spheres which are degassed in excess of their critical levels.

A model xenolith consisting of two types of spheres, retentive ($i = 1$) and nonretentive ($i = 2$), provides the simplest such example. We anticipate that type 1 spheres will have been degassed to $\tau_{e_1} < \tau_{crit}$, while type 2 spheres will have been degassed to $\tau_{e_2} > \tau_{crit}$ (Figure 3). The actual values of τ_{e_2} and τ_{e_1} will depend on a number of factors. Below we examine in detail the characteristics of the two kinds of spheres that permit the development of a plateau at t_x in the age spectrum. The question is whether plateaus at t_x can, in fact, be produced from model xenoliths containing two kinds of spheres, even if the degassing at t_e is only moderate, and whether this can be accomplished for spheres with reasonable ratios of a_1/a_2 or D_{0_1}/D_{0_2}, and reasonable values of Q_1 and Q_2. To facilitate this discussion the equations that describe the Ar budget may be simplified using the approximations of *Reichenberg* [1953] for $F(\tau)$, instead of the series of (4). These approximations are listed here for convenience:

$$F(\tau) = 6(\tau/\pi)^{1/2} \qquad F(\tau) \leq 0.1 \tag{16a}$$

$$F(\tau) = 6(\tau/\pi)^{1/2} - 3\tau \qquad F(\tau) \leq 0.9 \tag{16b}$$

$$F(\tau) = 1 - 6/\pi^2 \exp(-\pi^2\tau) \qquad F(\tau) > 0.9 \tag{16c}$$

For the present problem, the region of applicability of the approximations need not be sharply defined. For $\tau > 0.09$ ($F(\tau) \approx 0.75$), equations (16*b*) and (16*c*) differ by less than 0.006, while for $\tau < 0.005$ ($F(\tau) \approx 0.24$), equations (16*a*) and (16*b*) differ by less than 0.067.

Let the fraction of the total volume due to spheres of type 1 and type 2 be V_1 and V_2, respectively, with $V_1 + V_2 = 1$. As the amount of Ar loss for both types of spheres will generally be large at t_e, with losses from type 2 being virtually complete, it follows that (5) may be expressed as

$$F_p^{40}(t_e) \approx 1 - V_1 \frac{6}{\pi^2} \exp(-\pi^2\tau_{e_1}) \tag{17}$$

For the problem of interest, the fraction of ^{39}Ar loss due to heating at constant temperature in the laboratory (T_L) is not likely to be large before loss of residual original ^{40}Ar is significant. Therefore

$$F_p^{39}(t_L) \approx V_1(6(\tau_{L_1}/\pi)^{1/2} - 3\tau_{L_1}) + V_2(6(\tau_{L_2}/\pi)^{1/2} - 3\tau_{L_2}) \tag{18}$$

The expression for Z (equation (11*c*)) may thus be written

$$Z \approx \left\{ 2\sqrt{\pi}\, V_1 \exp[-\pi^2(\tau_{L_1} + \tau_{e_1})] \frac{d\tau_{L_1}}{dt_L} + 2\sqrt{\pi}\, V_2 \exp[-\pi^2(\tau_{L_2} + \tau_{e_2})] \frac{d\tau_{L_2}}{dt_L} \right\} \div \left[V_1(1/\sqrt{\tau_{L_1}} - \sqrt{\pi}) \frac{d\tau_{L_1}}{dt_L} + V_2(1/\sqrt{\tau_{L_2}} - \sqrt{\pi}) \frac{d\tau_{L_2}}{dt_L} \right] \tag{19}$$

Since T_L is constant

$$\frac{1}{\tau_{L_1}} \frac{d\tau_{L_1}}{dt_L} = \frac{1}{\tau_{L_2}} \frac{d\tau_{L_2}}{dt_L}$$

and if $\sqrt{\pi\tau_{L_2}} \ll 1$, equation (19) may be further simplified:

$$Z \approx \frac{12}{F_p^{39}(t_L)} [\tau_{L_1} V_1 \exp(-\pi^2\tau_{e_1}) + \tau_{L_2} V_2 \exp(-\pi^2\tau_{e_2})] \tag{20}$$

The condition for obtaining a plateau is $Z \leq \varepsilon t_x/t_0$ up to the time t_ε when $F_p^{39}(t_\varepsilon) = f$, which gives

$$12[\tau_{L_1} V_1 \exp(-\pi^2\tau_{e_1}) + \tau_{L_2} V_2 \exp(-\pi^2\tau_{e_2})] \approx f\varepsilon t_x/t_0 \tag{21a}$$

Due to the essentially complete loss of ^{40}Ar from the type 2 spheres at t_e, $\exp(-\pi^2\tau_{e_2})$ is negligible and

$$\tau_{L_1} V_1 \exp(-\pi^2\tau_{e_1}) t_0/t_x \approx f\varepsilon/12 \tag{21b}$$

From (17) we see also that

$$\tau_{L_1}[1 - F_p^{40}(t_e)]t_0/t_x \approx f\varepsilon/(2\pi^2) \qquad (21c)$$

Equation (21) in conjunction with (17) and (18) specifies the conditions for a plateau from a xenolith containing two types of spheres. A plateau of given characteristics f and ε may be achieved by a range of model xenoliths; for example, those with greater age t_0 must be degassed more thoroughly in the magma or must have retentive spheres (type 1) which are degassed less in the laboratory. Equation (18) shows that this latter condition can be achieved if τ_{L_2} is increased. Equation (17) shows that a given level of degassing in the magma $F_p^{40}(t_e)$ may be achieved by varying τ_{e_1} and V_1.

For a model xenolith of only one type of sphere we have $f \approx 6(\tau_{L_1}{}^*/\pi)^{1/2}$ and we obtain from (21a) $\tau_{e_1}{}^* = (1/\pi^2)[\ln(\pi f/3\varepsilon) - \ln(t_x/t_0)]$, where the asterisk indicates there are no other spheres in the model ($V_1 = 1$ and $V_2 = 0$). For such a model the level of degassing necessary to achieve the plateau is proportional to t_x/t_0. As noted earlier, for useful values of f, ε, t_x, and t_0, the parameter $\tau_{e_1}{}^*$ will be very large and may not be commonly achieved in nature.

For a plateau of fixed characteristics (f, ε, t_x, t_0) the values of τ_{L_1} and τ_{e_1} for the two-sphere ($V_1 < 1$) and one-sphere models ($V_1 = 1$) are approximately related through (21b):

$$\ln(\tau_{L_1}{}^*/\tau_{L_1}) \approx \pi^2(\tau_{e_1}{}^* - \tau_{e_1}) + \ln V_1 \qquad (22)$$

This relation is shown in Figure 4 for three different values of V_1. The case where $V_1 = 1$ plots at the origin. As the fractional volume of retentive spheres V_1 is reduced from unity, the diffusion necessary to achieve the plateau will always be reduced from $\tau_{e_1}{}^*$. This corresponds to a reduction of $F_p^{40}(t_e)$, the overall degassing of the xenolith in the magma, compared to the one-sphere model. Thus a two-sphere model xenolith may produce a plateau at t_x even if it is not as extensively degassed as a one-sphere model. The reduction from $\tau_{e_1}{}^*$ need not be accompanied by a reduction in τ_{L_1} (degassing of the retentive spheres in the laboratory), but, in general, this will be the case. The special case where $\tau_{L_1} = \tau_{L_1}{}^*$ corresponds to the minimum disparity between the two types of spheres. The disparity between sphere types 1 and 2 is found in terms of τ_{L_2}/τ_{L_1} through (18). For models of a given V_1, the farther from the origin the model plots, the less τ_{e_1} and τ_{L_1} are, and the greater τ_{L_2}/τ_{L_1} must be. It should be recalled that the above equations are approximate and apply well only to a limited range of τ_{L_1}, τ_{L_2}, τ_{e_1}, and τ_{e_2}.

It remains to be shown that the reduction in degassing of the two-sphere model xenolith is large enough that a xenolith of realistic characteristics (a, D_0, and Q) degassed to levels actually observed would yield a plateau at t_x. *Dalrymple* [1964] has reported granitic xenoliths degassed in a basaltic lava to $F_p^{40}(t_e) > 95\%$. Representative values of τ_{L_1}/τ_{L_2} calculated approximately from (21c) and (18) may be used to specify the ranges of physical parameters a, D_0, and Q for which plateaus at t_x can be anticipated. For $f = 0.25$ (a 25% plateau), $\varepsilon = 0.05$, $t_x = 10^6$ years, and $t_0 = 10^8$ years, we get $\tau_{L_1} = 6.3 \times 10^{-6}\,[1 - F_p^{40}(t_e)]^{-1}$. For a population with $F_p^{40}(t_e) = 0.95$ (95% loss from the xenolith), we get $\tau_{L_1} = 1.3 \times 10^{-4}$, which corresponds to a 4% loss of ^{39}Ar from the retentive (type 1) spheres. If V_1 is also specified, the other important parameters may be found from (17) and (18). For $V_1 = 0.5$, $\tau_{e_1} = 0.18$ and $\tau_{L_2} = 2.5 \times 10^{-2}$. This corresponds to a 46% loss of ^{39}Ar from the nonretentive type 2 spheres at the time the plateau is completed. Thus $\tau_{L_2}/\tau_{L_1} = 192$, which requires that $D_{0_2}/D_{0_1} = 192$ or that $\exp[(Q_1 - Q_2)/RT_L] = 192$ or that the grain sizes differ by a factor of 14. If the ratio τ_{L_2}/τ_{L_1} is governed by the activation energy, we obtain $Q_1 - Q_2 = 11$ kcal/mol for $T_L = 1100$ K. If $F_p^{40}(t_e)$ is reduced to 0.9, τ_{L_2}/τ_{L_1} is increased from 192 to 429. Approximate calculations such as these permit easy analysis of possible conditions for obtaining plateaus at t_x for bimodal distributions of spheres.

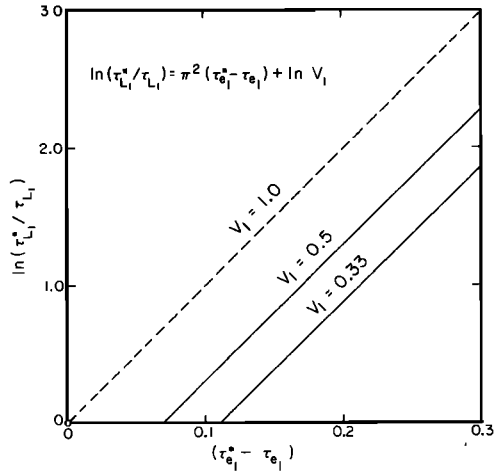

Fig. 4. For model xenoliths containing two types of spheres, the degassing of the retentive spheres (type 1) in the magma ($F^{40}(\tau_{e_1})$) and in the laboratory ($F^{40}(\tau_{L_1})$) required to yield a low-temperature plateau at t_x are both reduced compared to the equivalent parameters $F^{40}(\tau_{e_1}{}^*)$ and $F^{40}(\tau_{L_1}{}^*)$ which describe the model xenolith consisting entirely of type 1 spheres ($V_1 = 1$). The figure shows lines relating $(\tau_{e_1}{}^* - \tau_{e_1})$ and $\ln(\tau_{L_1}{}^*/\tau_{L_1})$ for three values of V_1. For $V_1 = 1$, the relation is degenerate since then $\tau_{L_1} = \tau_{L_1}{}^*$ and $\tau_{e_1} = \tau_{e_1}{}^*$. This case plots at the origin. The dashed line for $V_1 = 1$ is the limit as V_1 approaches unity.

In the above discussion, T_L was taken to be constant. This is not typical of most laboratory extraction schedules; T_L is generally increased between steps, and this results in a different value of Q/RT_L for each step. If $Q_1 \neq Q_2$, then (τ_{L_2}/τ_{L_1}) depends in part on the heating schedule. However, for realistic heating schedules the effect on (τ_{L_2}/τ_{L_1}) at t_ε is not large, because most Ar loss occurs in the step with the highest T_L. The effect of increasing T_L at fixed intervals (Δt) by 100-K increments to 1000 K, compared to extracting Ar in one longer step at 1000 K, is to increase (τ_{L_2}/τ_{L_1}) by ~12%, for realistic values of Q_1 and Q_2 (~20 to ~100 kcal/mol). Thus the above discussion applies in a general way to laboratory extractions with variable T_L.

2.1. *Some Illustrative $dN_{Op}{}^{40}/dN_p{}^{39}$ Spectra*

We next illustrate with specific examples of model xenoliths the relationship among the parameters a, Q, and V_1 and the formation and degassing history given by t_0, t_x, and $F_p^{40}(t_e)$. In the subsequent section we discuss the effect of variation in these parameters on the characteristic f (equation (15)) of the age spectra from model xenoliths. In contrast to the discussion above, the exact expressions (1)–(15) and a realistic laboratory heating schedule were used to calculate the ^{40}Ar-^{39}Ar spectra.

Figure 5 shows the $dN_{Op}{}^{40}/dN_p{}^{39}$ spectra obtained for model xenoliths composed of bimodal populations of spheres stepwise degassed at increasingly higher temperatures. The continuous spectra were approximated by spectra

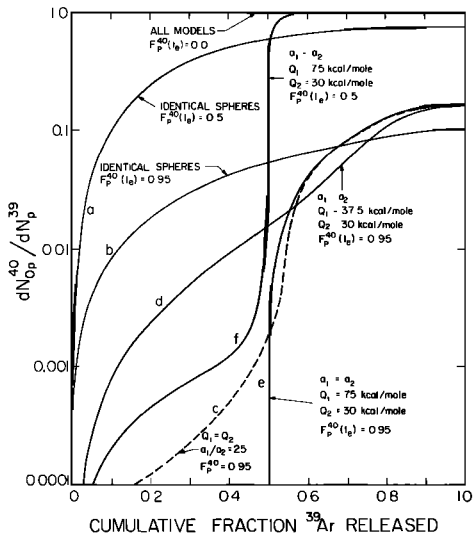

Fig. 5. Values of dN_{Op}^{40}/dN_p^{39} as a function of $F_p^{39}(t_L)$, the cumulative fraction of ^{39}Ar released from different model xenoliths partially degassed of ^{40}Ar in magma just before ^{40}Ar-^{39}Ar analysis. Analysis was taken to have immediately followed cooling of the magma ($t_x = t_e$), so that the ^{40}Ar degassed from the model xenoliths was all residual original ^{40}Ar. Examples of spectra from three types of model xenoliths are shown: (1) identical spheres (curves 'a' and 'b'), (2) equal volumes of two types of grains of different radii a_1 and a_2 ('c'), and (3) equal volumes of two types of grains of different activation energies Q_1 and Q_2 ('d,' 'e,' and 'f'). The different values of a_1/a_2, Q_1 and Q_2, and the fraction of original ^{40}Ar degassed in the magma ($F_p^{40}(t_e)$) are indicated in the figure. Even in the case that samples of identical spheres are heavily degassed, contributions of residual original ^{40}Ar are negligible only for the first small fraction of ^{39}Ar released. On the other hand, the amount of residual original ^{40}Ar released from model xenoliths consisting of two types of grains with only moderate differences in Q may be negligible over a substantial fraction of the ^{39}Ar released if $F_p^{40}(t_e)$ is as large as 0.95. Similar results are obtained if the sample contains spheres of highly different radii. Plateaus of similar extent may be achieved if $F_p^{40}(t_e)$ is as small as 0.5, as long as Q_1 and Q_2 or a_1 and a_2 are sufficiently different.

of $\delta N_{Op}^{40}/\delta N_p^{39}$ calculated assuming that the extraction occurred in small but finite steps of 360-s duration. The beginning temperature was T_L = 300 K; the increment of T_L was 10 K. The stepped spectra have been smoothed for simplicity. Degassing in the lava was assumed to have occurred at T_e = 1400 K. We further assumed that $t_x = t_e$, so that $C_N^{40} = 0$. For simplicity, all spheres were assumed to have $D_0 = 1$; thus discussion is in terms of grain radius a rather than $a/\sqrt{D_0}$.

Spectra of dN_{Op}^{40}/dN_p^{39} from examples of each of three categories of models are shown in Figure 5: (1) identical spheres (curves 'a' and 'b'), (2) spheres of two different radii a_1 and a_2 but the same activation energy ('c'), and (3) spheres of the same radius but two different activation energies Q_1 and Q_2 ('d,' 'e,' and 'f'). For categories 2 and 3, V_1 was taken to be 0.5. The examples provide simple illustrations of the effects of grain size and activation energy distributions on age spectra. These curves are related to differential age spectra through (12). Age t_0 corresponds to $dN_{Op}^{40}/dN_p^{39} = 1.0$. For $t_0 = 10^8$ years, the age is proportional to dN_{Op}^{40}/dN_p^{39} within 3%. Lesser values of dN_{Op}^{40}/dN_p^{39} reflect Ar loss during heating in the magma. If there was no loss of Ar during heating in the magma ($F_p^{40}(t_e) = 0$), the measured age would be independent of $F_p^{39}(t_L)$. The spectrum would consist of a plateau corresponding to t_0, the age of crystallization. This general case is shown in Figure 5. Details of the six other examples and their spectra are given below.

Curve 'a' shows dN_{Op}^{40}/dN_p^{39} versus $F_p^{39}(t_L)$ calculated for identical spheres from which 50% of the original ^{40}Ar was degassed in the magma ($F_p^{40}(t_e) = 0.5$). Values of dN_{Op}^{40}/dN_p^{39} rise swiftly for $F_p^{39}(t_L) < 0.2$ and exceed 0.01 after only ~2% of the ^{39}Ar has been released. The maximum value of 0.74 is achieved for the last fraction of ^{39}Ar extracted. No fraction of Ar is completely devoid of original ^{40}Ar, and all fractions are seriously depleted in original ^{40}Ar compared to the case where $F_p^{40}(t_e) = 0$.

Curve 'b' was calculated for identical spheres for which $F_p^{40}(t_e) = 0.95$. The shape of 'b' is similar to 'a,' and although the maximum value of dN_{Op}^{40}/dN_p^{39} is reduced nearly an order of magnitude, the fraction of ^{39}Ar released before $dN_{Op}^{40}/dN_p^{39} = 0.01$ is only ~0.12. Thus it appears that virtually all ($\gg$95%) the original ^{40}Ar must be degassed from a sphere or group of identical spheres before a sizable fraction of ^{39}Ar can be extracted without significant contributions of original ^{40}Ar.

We next examine instances in which populations of different spheres are analyzed. Curve 'c' was calculated for a population of spheres having the same activation energy but two greatly different radii $a_1 = 25a_2$. Few real systems will have grain populations with this difference in sizes. The total volume of spheres of each kind was assumed to be equal ($V_1 = 0.5$), and τ_{e_1} was fixed at 0.183, such that $F_p^{40}(t_e) = 0.95$. This corresponds to degassing in the magma of 90% of the original ^{40}Ar from spheres of radius a_1 and degassing of essentially 100% of the initial ^{40}Ar from original spheres of radius a_2. The spectrum is grossly different from 'a' and 'b.' Values of dN_{Op}^{40}/dN_p^{39} rise more slowly at low values of $F_p^{39}(t_L)$ and over half the ^{39}Ar is extracted before $dN_{Op}^{40}/dN_p^{39} = 0.01$. Ar represented by the first part of the spectrum was derived largely from the nonretentive type 2 grains. For $F_p^{39}(t_L) > 0.5$, values of dN_{Op}^{40}/dN_p^{39} rise steeply before finally leveling off. Ar for the last part of the spectrum was extracted largely from the retentive type 1 grains. The maximum value of dN_{Op}^{40}/dN_p^{39} is 0.16 and occurs when $F_p^{39}(t_L) = 1.0$. From the sigmoidal shape of the spectrum, it is clear that degassing from the large grains begins only after the small ones are nearly exhausted, and in fact, the amount of original ^{40}Ar released for $F_p^{39}(t_L) < 0.5$ is as much as 2 orders of magnitude less than that from model 'b' at equivalent values of $F_p^{39}(t_L)$.

The values of dN_{Op}^{40}/dN_p^{39} for $F_p^{39}(t_L) < V_2$ are very sensitive to the exact value of $F^{40}(\tau_{e_2})$ for the smaller spheres. For example 'c,' this value was actually 0.99996 rather than 1.00 exactly. If the smaller spheres were truly completely degassed, then the amount of original ^{40}Ar released when $F_p^{39}(t_L) < 0.5$ would be orders of magnitude smaller. For spheres of $a_1 = 25a_2$, this cannot be achieved if $F_p^{40}(t_e)$ is to be maintained at 0.95, but it can be achieved by further increasing the disparity in the sizes of the spheres. The spectrum for $F_p^{39}(t_L) > 0.5$ would vary little if a_1/a_2 were increased. If a_1/a_2 were decreased, the spectrum would rapidly approach curve 'b.'

Curve 'd' was calculated for a model xenolith containing spheres of the same size but Q = 37.5 kcal/mol and Q_2 = 30 kcal/mol. Degassing of ^{40}Ar in the magma was 95% complete ($F_p^{40}(t_e) = 0.95$), which as before resulted from nearly

complete degassing of the nonretentive spheres and degassing of the retentive spheres to $F^{40}(\tau_{e_1}) = 0.9$.

Curve 'd' is intermediate to 'b' and 'c' in appearance. Values of dN_{Op}^{40}/dN_p^{39} rise less steeply than for 'b' and do not exceed 0.01 until $F_p^{39}(t_L) > 0.4$. The sigmoidal shape seen in 'c' is not pronounced, and at $F_p^{39}(t_L) = 1.0$, dN_{Op}^{40}/dN_p^{39} has the same value (0.16) as for curve 'c.' Since T is increased during laboratory analysis, the diffusivities for spheres of different Q will become less disparate with increasing $F_p^{39}(t_L)$, whereas the diffusivities for spheres of different radii (but the same Q) will maintain their relative values. At $T = 500$ K, model xenolith 'd' degasses as model 'c' with $a_1/a_2 = 44$, and at $T = 1400$ K as model 'c' with $a_1/a_2 = 4$. Within that temperature range the spectrum is intermediate between the spectra of those two end-members. However, because degassing is inefficient at low temperatures, for most of the analysis ($F_p^{39}(t_L) > 0.05$) the spectrum is close to that for model 'c' with $4 < a_1/a_2 < 6$.

For model 'd' it was marginally possible to extract a significant fraction of the ^{39}Ar unaccompanied by large amounts of residual ^{40}Ar. This fraction can be increased by increasing the disparity between the two activation energies, keeping the total degassing in the magma $F_p^{40}(t_e)$ fixed. An extreme example was chosen for model 'e' to illustrate this point. Q_1 was increased to 75 kcal/mol, but degassing in the magma was maintained at 95% ($F_p^{40}(t_e) = 0.95$). The change in the spectrum was profound (curve 'e'). Original ^{40}Ar released when $F_p^{39}(t_L) < 0.5$ was more than 4 orders of magnitude lower than if $F_p^{40}(t_e) = 0$. Nevertheless, the maximum value of the spectrum (0.16) was unchanged.

Curves 'd' and 'e' illustrate that with a xenolith of appropriate properties it is possible that for at least a sizable fraction of the ^{39}Ar released, dN_{Op}^{40}/dt_L might be sufficiently small to permit the measurement of the age of eruption even if $t_x/t_0 = 0.01$.

Curve 'f' was calculated as for case 'e' except that $F_p^{40}(t_e) = 0.50$. This spectrum differs from all others in that for the first half of the spectrum the release of original ^{40}Ar is minimal and for the second half it is virtually undiminished by the heating in the magma. For $F_p^{39}(t_L) < 0.4$, $dN_{Op}^{40}/dN_p^{39} < 0.001$, and for $F_p^{39}(t_L) > 0.6$, $dN_{Op}^{40}/dN_p^{39} = 1.0$. Thus for a xenolith described by this model, it might be possible to find two plateaus in the same spectrum, one at t_x, the age of eruption, and one at t_0, the age of original crystallization.

In Figure 6 we show the age spectra for five of the models of Figure 5, for the special case where $t_0 = 10^8$ years and $t_x = 10^6$ years. The same letters are used in both Figures 5 and 6 to identify spectra from the same models.

The age spectrum for model 'a' rises rapidly from a minimum age of 1 m.y. to a maximum of 75 m.y. No age plateau is developed, so that neither t_x nor t_0 can be determined. Even though the maximum apparent age for model 'b' is only 9.4 m.y., again no plateau is developed. After only 5% of the ^{39}Ar has been released, residual ^{40}Ar contributions increase the apparent age from 1 m.y. (at $F_p^{39}(t_L) = 0$) to 1.4 m.y. Even when $F_p^{39}(t) = 0.01$, the apparent age of 1.1 m.y. is already 10% greater than the age of eruption. For the case illustrated, to achieve an age plateau of $f = 0.25$ and $\varepsilon = 0.05$ would require $F_p^{40}(t_e) > 0.999$. On the other hand, dN_{Op}^{40}/dt_L is essentially zero for the infinitesimal fraction of ^{39}Ar released, so that even for identical spheres an upper limit to the age of eruption should in theory be measurable regardless of $F_p^{40}(t_e)$, as long as $\tau_e \neq 0$.

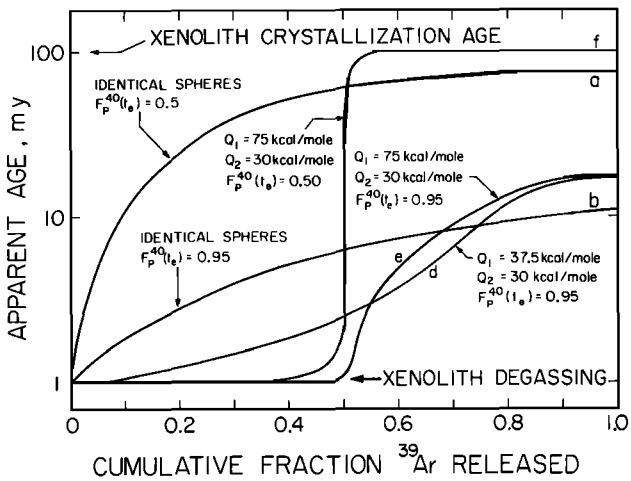

Fig. 6. Apparent age as a function of ^{39}Ar released from samples crystallized 100 m.y. ago and partially degassed of ^{40}Ar 1 m.y. ago. Letters on curves refer to the same models as in Figure 5. The age spectra here differ from the dN_{Op}^{40}/dN_p^{39} spectra of Figure 5 due to the uniform accumulation of new ^{40}Ar from $t = t_e$ to $t = t_x$. In the case of identical spheres, essentially all ^{40}Ar must be degassed in the magma to achieve low-temperature plateaus of any size. However, extensive low-temperature plateaus corresponding to the age of eruption can be achieved for xenoliths with a gross difference in grain sizes or a small difference in activation energies.

It was seen from Figure 5 that model xenoliths consisting of spheres of more than one radius or activation energy were a prerequisite for the development of well-defined low-temperature plateaus giving t_x. Curve 'd' in Figure 6 is the age spectrum for the model xenolith with spheres of $Q_1 = 37.5$ kcal/mol and $Q_2 = 30$ kcal/mol. The maximum apparent age is 17 m.y., and the apparent age exceeds the age of eruption by 5% after release of only 7% of the ^{39}Ar. At this time the model temperature T_L was 1050 K. Using the approximate equations (17), (18), and (21c) together with the Arrhenius relation (equation (2)), we find for the isothermal case with $T_L = 1050$ K that $f \approx 0.069$, which is in close agreement with the value calculated exactly ($f = 0.072$). Spectrum 'd' is probably inadequate to determine the age of eruption but would certainly provide a closer limit to the eruption age than either 'a' or 'b.'

Age spectrum 'e' shows that the effect of increasing Q_1 to 75 kcal/mol is to increase f sevenfold, if $\varepsilon = 0.05$. For such a xenolith the age of eruption could certainly be determined.

Curve 'f,' calculated for the same model used for 'e' but degassed only 50%, shows that two plateaus might be observed if $t_0/t_x \leq 100$. The low-temperature plateau extends over the first 35% of ^{39}Ar released before the apparent age rises to 1.05 m.y. It can be used to define the age of eruption (t_x). The high-temperature plateau, which defines the age of original crystallization (t_0), extends over the last 45% of the ^{39}Ar extracted. To achieve a comparable spectrum for a model xenolith with $Q_1 = Q_2$ but $a_1 \neq a_2$ would require $a_1/a_2 \gg 100$.

2.2. *The Extent of the Plateaus Corresponding to the Age of Eruption*

Figure 7 shows $f = F_p^{39}(t_\varepsilon)$ for eruption age plateaus as a function of four parameters: (1) the fraction of ^{40}Ar degassed

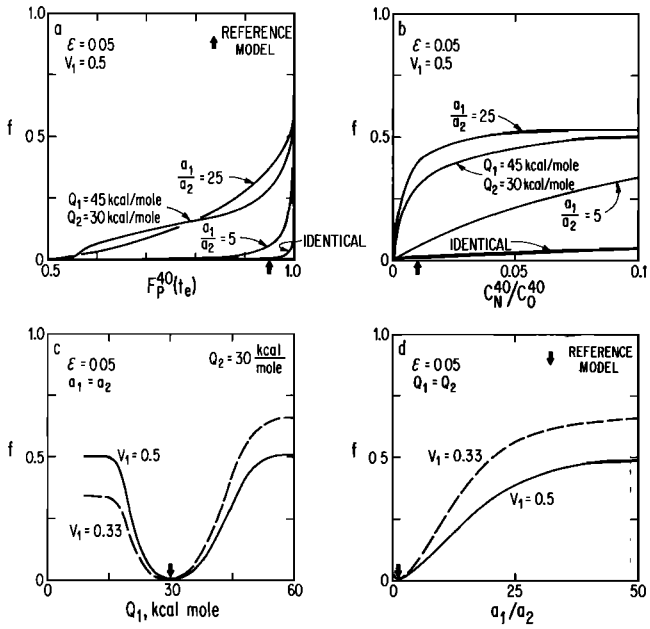

Fig. 7. The fraction f of ^{39}Ar defining the eruption age plateau in the ^{40}Ar-^{39}Ar age spectrum as a function of (*a*) the fraction of original ^{40}Ar degassed by the lava, (*b*) the relative amounts of ^{40}Ar accumulated in the model xenolith before and after eruption of the lava, and (*c*) and (*d*) the characteristics of sites in the model xenolith occupied by the Ar. ε is the maximum fractional deviation of measured age from the actual eruption age (or C_N^{40}/C^{39}). The model xenolith consists of spheres of the same K concentration, bimodally distributed according to radius a or activation energy Q. Q_2 was always taken to be 30 kcal/mol. The laboratory heating schedule was taken to be the same as for Figures 5 and 6. The reference xenolith, designated by arrows in the figures, consists of identical spheres ($a_1 = a_2$, $Q_1 = Q_2$) with $C_N^{40}/C_O^{40} = 0.01$. Figure 7*a* demonstrates that f increases as $F_p^{40}(t_e)$, a_1/a_2, or $|Q_1 - Q_2|$ is increased. Values of $a_1/a_2 = 25$, $Q_1 = 45$ kcal/mol and $Q_2 = 30$ kcal/mol were selected to show that plateaus of $f > 0.25$ can be achieved for Cretaceous xenoliths degassed 95% in a Pleistocene lava. The value of f decreases strongly for these models if $C_N^{40}/C_O^{40} < 0.01$ (Figure 7*b*), as activation energies for the two spheres of the model become more similar (Figure 7*c*), or as a_1/a_2 approaches unity (Figure 7*d*). For $Q_1 < 18$ kcal/mol or $Q_1 > 54$ kcal/mol and for $a_1/a_2 \gtrsim 25$ little further increase in f is achieved. The value of f reaches an upper limit V_2 (or $1 - V_1$), which is the fraction of ^{39}Ar from the nonretentive spheres.

from the sample at the time of eruption ($F_p^{40}(t_e)$), (2) the ratio of concentration of new ^{40}Ar accumulated since the time of degassing (C_N^{40}) to the concentration which had accumulated by the time of degassing (C_O^{40}), which is approximately the same as the ratio of ages t_x/t_0, (3) the difference in activation energies for diffusion from distinct Ar reservoirs in the sample (with $Q_2 = 30$ kcal/mol), and (4) the ratio a_1/a_2 of grain sizes for diffusion from different reservoirs in the sample. Again, we assume all spheres have identical K content and $D_0 = 1$. In each graph a reference model consisting of identical spheres for which $F_p^{40}(t_e) = 0.95$ is indicated by an arrow. These reference model spheres contain new and original ^{40}Ar in the ratio $C_N^{40}/C_O^{40} = 0.01$. For simplicity, ε has been set to 0.05. Curves in Figure 7 were calculated for $V_1 = 0.5$ and $V_1 = 0.33$. Otherwise, the model is the same as described for Figure 5. The results in Figure 7 generalize the examples of section 2.1.

Figure 7*a* shows that f increases with $F_p^{40}(t_e)$. For the reference model, $f \approx 0.01$ and no plateau at t_x would be identified. Not unless $f \approx 0.25$ could a plateau be reliably identified in experimental data. For the model consisting of identical spheres this would not be achieved until $F_p^{40}(t_e) > 0.999$. Other curves in Figure 7*a* show that less degassing in the magma is necessary to achieve a given f if the xenolith contains spheres of different radii or activation energies. If $a_1/a_2 = 5$, $F_p^{40}(t_e) \approx 0.99$ is still required for $f = 0.25$; but if $a_1/a_2 = 25$, only $F_p^{40}(t_e) = 0.87$ is necessary. If $a_1 = a_2$ but $Q_1 = 45$ kcal/mol and $Q_2 = 30$ kcal/mol, a curve similar to that for $a_1/a_2 = 25$ is obtained.

Dalrymple [1964] has shown that degassing of granitic xenoliths in basalt in some instances exceeds 95%. Degassing at this level would be sufficient to permit the development of plateaus in the ^{40}Ar-^{39}Ar age spectra of xenoliths at the age of degassing or eruption as long as the xenoliths were characterized by Ar in lattice sites of two or more sufficiently different diffusion radii or activation energies.

Figure 7*b* shows the sensitivity of f to the ratio of the age of eruption of the host lava and the original age of crystallization of the xenolith. This ratio is here represented by C_N^{40}/C_O^{40}; f increases with C_N^{40}/C_O^{40} because the sample must be more extensively degassed in the laboratory if it is to release new and original ^{40}Ar in a fixed ratio at a fixed $F_p^{39}(t_L)$ when C_N^{40} is increased with respect to C_O^{40}. Even when $C_N^{40}/C_O^{40} = 0.1$, a model containing only identical spheres cannot produce a spectrum with $f > 0.05$; f is again greater for the other three models from Figure 7*a*. If $a_1/a_2 = 5$, $f > 0.25$ is achieved for $C_N^{40}/C_O^{40} > 0.06$. If $a_1/a_2 = 25$ or if $Q_1 = 45$ kcal/mol and $Q_2 = 30$ kcal/mol, $f > 0.25$ can be achieved even if $C_N^{40}/C_O^{40} < 0.01$. For both of these models, f approaches a limiting value reflecting the value of V_1 chosen for the model. For $V_1 = 0.5$, f cannot be significantly larger than 0.5 unless the retentive spheres also are virtually depleted of original ^{40}Ar.

Figure 7*c* shows the dependence of f on Q_1 and Q_2 for $V_1 = 0.5$ and $V_1 = 0.33$. If $Q_1 > 54$ kcal/mol or if $Q_1 < 15$ kcal/mol ($Q_2 = 30$ kcal/mol), $f = 0.5$ can be achieved even if $F_p^{40}(t_e)$ is only 0.95. Degassing of new ^{40}Ar from the nonretentive spheres then occurs at temperatures low enough that residual original ^{40}Ar from the other spheres is retained. Only at high extraction temperatures, when the nonretentive spheres are depleted, does degassing of the retentive spheres begin. For values Q_1 closer to Q_2, degassing of the two populations of spheres occurs at more comparable temperatures, and less new ^{40}Ar is released unaccompanied by residual ^{40}Ar. If 21 kcal/mol $< Q_1 <$ 44 kcal/mol, then $f < 0.25$.

The graphed range of Q_1, 9 to 60 kcal/mol, includes most published activation energies for K-feldspars. Thus real xenoliths containing two types of feldspar could yield age spectra with $f > 0.25$.

Figure 7*d* shows the increase of f with a_1/a_2. Limiting values of f are V_1 for $a_1 > a_2$, just as for the two-Q model. For $V_1 = 0.33$, $f > 0.25$ is attained if $a_1/a_2 > 10$. Such a disparity in the characteristic diffusion dimension might be seen in a feldspar if a were determined by the size of exsolution lamellae. Differences in values of Q required to develop plateaus in age spectra are much smaller than differences in values of a required to develop plateaus of equivalent f.

2.3. *Discussion*

The shape of an age spectrum from a model xenolith and the amount of useful information conveyed by it depend strongly on the model parameters from which it was calculat-

ed. For a xenolith composed of identical spheres, it is not reasonable to expect an age plateau of any size unless $t_x/t_0 \gg 0.01$ or unless degassing was essentially complete. On the other hand, model xenoliths consisting of spheres of very different sizes or somewhat different activation energies can produce age spectra containing plateaus identifying both the eruption and crystallization ages even if $t_x/t_0 < 0.01$. Thus a Pleistocene basalt might be datable by ^{40}Ar-^{39}Ar analysis of an included Cretaceous xenolith.

Most actual samples will have a distribution in grain size and, if consisting of more than one phase, a distribution in activation energy. It is evident from Figures 7*c* and 7*d* that unless either the age of crystallization and the time of eruption were comparable or degassing in the magma essentially complete, distributions of a and Q would be necessary if a meaningful eruption age were to be determined. Values of $f > 0.25$ can be obtained if major reservoirs of ^{40}Ar in the sample differ by a factor of 10 or more in grain size (Figure 7*d*) or by only 12 kcal/mol or more in activation energy (if one activation energy is 30 kcal/mol). A factor of 2 difference in Q or extreme disparity in a may result in essentially complete degassing of one reservoir and a value for f comparable to the fraction of ^{40}Ar held in that reservoir, even though degassing of the total system may be relatively low. It can also be concluded that if a large f for any eruption age plateau is observed, it is likely to imply a distribution in Q or a, given the difficulty of achieving large f with a sample composed of comparably sized grains. As expected, it becomes rapidly more difficult to achieve large f as the fraction of ^{40}Ar degassed in the magma becomes smaller or as the eruption age and crystallization age become more disparate. It is also clear from the figures that sufficiently large f can be achieved by a combination of factors, so that variations in one parameter need not be so extreme.

Activation energies of 18 and 24 kcal/mol have been reported by *Evernden et al.* [1960] for microcline, and activation energies of 52 kcal/mol [*Baadsgaard et al.*, 1961] and 56 kcal/mol [*Fechtig et al.*, 1960] have been reported for sanidine and anorthite, respectively. Consequently, substantial differences in Q could be expected for real samples containing two feldspars, and we anticipate that plateaus at t_x would be found in such samples, provided degassing in the magma exceeded ~90%.

That $F_p^{40}(t_e) > 0.9$ can be achieved in natural samples is shown by calculating τ using a realistic thermal history $T(t)$ of a xenolith in a magma and the Arrhenius equation. Ar retention in the xenolith may then be estimated from (4) and (5). At the center of a spherical xenolith in a well-stirred magma, the thermal history is given by *Carslaw and Jaeger* [1959] as

$$T_c(t) = T_e + 2T_e \sum_{n=1}^{\infty} (-1)^n e^{-\kappa n^2 \pi^2 t/a^2} \qquad (23)$$

where T_c is the temperature at the xenolith center, T_e is the magma temperature, a is the xenolith radius, and κ is the thermal diffusivity of the xenolith. If $\kappa = 0.01$ cm^2/s and $T_e = 1100$°C, T_c rises from 0°C to 1050°C after only 40 s for a 1-cm xenolith. This might easily be achieved during incorporation of the inclusion in the erupting lava. Temperatures exceeding 1050°C might be expected for days or months, depending on the dimensions of the flow. The amount of degassing from a xenolith in such an environment can be estimated. For orthoclase, *Foland* [1974] determined $D_0/a^2 \approx 245$ s^{-1} and $Q = 43.8$ kcal/mol, so that $\tau > 1.4$ if $T = 1050$°C for 10^5 s. Thus for a spherical orthoclase xenocryst, $F^{40} > 0.99$ (however, if $Q = 49.2$ kcal/mol, $F^{40} = 0.9$). We conclude from model behavior alone that degassing in magma is probably sufficient to permit measurement of eruption age plateaus for at least some granitic xenoliths. This theoretical conclusion is consistent with the ^{40}Ar retention of 3% in a granitic xenolith measured by *Dalrymple* [1964].

The ability to extract useful dates from polymineralic whole rock systems is implied by our models, provided that individual reservoirs of Ar are sufficiently distinct in a or Q. This removes the requirement to separate carefully minerals before analysis. However, the most reliable age of eruption or degassing would still be determined from analysis of minerals containing only reservoirs depleted of Ar during heating in the magma.

3. Experimental Confirmation

To test the ability of granitic xenoliths from basic lava flows to yield the date of eruption in ^{40}Ar-^{39}Ar age spectra, a quartz monzonite xenolith from an early Pleistocene lava flow from the Sierra Nevada, California, was analyzed. The lava was an alkalic olivine basalt which we found to have about 1.4% K (by weight). The xenolith (NFOC-1), about 1 cm in diameter, was apparently derived from the late Cretaceous McGann pluton. *Moore* [1963] reported that samples of the McGann quartz monzonite averaged 3% hornblende, 7% biotite, 36% each of K-feldspar (microcline) and plagioclose, and 17% quartz. The grain size in the xenolith was from 1 to 2 mm. In thin section, a few microcline crystals appeared to have been transformed to sanidine; at the xenolith-basalt interface, quartz crystals were corroded and showed reaction rims of clinopyroxene needles. The xenolith was readily crushed with a hammer. However, the microcline crystals appeared fresh and unaltered.

The xenolith was gently crushed in a stainless steel mortar and sieved. The 100–220 μm fraction was then magnetically cleaned of its mafic minerals. About 0.5 g of the remaining grains were sealed in an Al foil packet and irradiated with a fast neutron fluence of ~10^{17} n cm^{-2} in the TRIGA reactor facility of the U.S. Geological Survey at Denver, Colorado. Neutron fluence inhomogeneities were monitored by measuring the ^{58}Co$_\gamma$ activity induced in Ni wires placed between samples. The Bern 4M standard muscovite [*Jäger et al.*, 1963] was used as the neutron irradiation monitor, along with samples of CaF_2 to measure Ar isotopes produced from Ca. The age of the muscovite was taken to be 17.9 ± 0.6 m.y., the result of ^{40}Ar-^{39}Ar analysis reported by *Dalrymple and Lanphere* [1971] corrected for the ^{40}K isotopic abundance estimate and decay constant $\lambda = 5.43 \times 10^{-10}$ year^{-1} recommended by *Steiger and Jäger* [1977].

After neutron irradiation, Ar was extracted from the sample in 15 one-hour steps at successively higher temperatures from 300°C to 1700°C. The sample was heated in a W crucible by RF induction. Blank levels of ^{36}Ar were about 10^{-10} cm^3 STP at temperatures below 800°C, and rose to 10^{-8} cm^3 STP at 1700°C. Blank Ar was of atmospheric composition.

Ar extracted from the sample was purified and then analyzed, using the HENEAK II gas mass spectrometer with programmed magnetic field scanning. Because only about 10^{-7} cm^3 STP/g radiogenic ^{40}Ar was present in the xenolith, an electron multiplier was required to measure ^{36}Ar ion currents. Details of the Ar analysis and corrections for

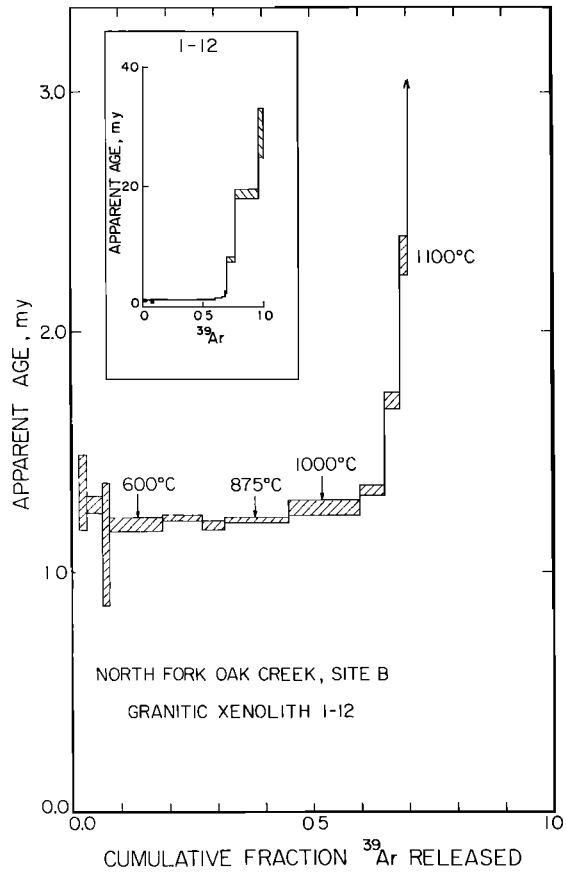

Fig. 8. Apparent age spectrum for a xenolith from a Cretaceous quartz monzonite pluton which was found in an early Pleistocene basalt ($t_x/t_0 \approx 0.01$). The spectrum exhibits an extensive plateau encompassing at least 60% of the ^{39}Ar extracted. The steep rise in apparent age for Ar released above 1000°C is caused by the presence of residual original ^{40}Ar that was not degassed during heating in the basaltic magma. The inset shows at reduced scale the entire age spectrum. The maximum age of ~30 m.y. is less than the age of original crystallization of ~100 m.y. The plateau identifies the age of eruption (~1.2 m.y.). Extensive plateaus such as this are found in age spectra from model xenoliths characterized by multiple diffusion sites of different a or Q. The error bars are 1σ.

interference isotopes have recently been reported by *Radicati di Brozolo et al.* [1981] and will not be repeated here. Data are given by *Gillespie* [1982] and are available from the authors. Complete results will be discussed in a later paper (A. R. Gillespie et al., manuscript in preparation, 1982).

3.1. ^{40}Ar-^{39}Ar Age Spectrum

The age spectrum determined for xenolith 1–12 is presented in Figure 8. Ar from the first step was close to atmospheric Ar in composition and the uncertainty in the age (not plotted) was excessive. The subsequent eight extraction steps at temperatures up to 1000°C yielded Ar from which similar apparent ages of about 1.2 m.y. were calculated. Nearly 60% of the total ^{39}Ar was released during these steps. At extraction temperatures above 1000°C the Ar was increasingly dominated by radiogenic ^{40}Ar with greater ^{40}Ar/^{39}Ar. This ^{40}Ar caused a striking rise in the apparent age to a maximum of about 30 m.y. for the final step (at 1700°C). Thus the age spectrum is characterized by a large plateau extending over the first 60% of the ^{39}Ar release and a steep increase in apparent ages in the final 40%. Together, the eight steps of the low-temperature plateau define an age of 1.19 ± 0.05 (2σ) m. y. The total age calculated for all the Ar extracted from the sample was about 6.5 m.y.

3.2. Discussion

If the xenolith originally crystallized 100 m.y. ago, then it lost about 95% of its radiogenic ^{40}Ar upon incorporation in the magma. The maximum apparent age measured, ~30 m.y., is not close to the crystallization age, and no hint of an age plateau is seen for Ar extracted at high temperatures (>1000°C). On the other hand, the age of 1.2 m.y. indicated by the plateau defined by Ar extracted at temperatures below 1000°C is a reasonable one for the basalt, which was shown by *Moore* [1963] to have been erupted before the late Pleistocene glaciations.

The ^{39}Ar release pattern for sample 1–12 exhibits three release peaks with increasing temperature, indicating multiple siting of the ^{39}Ar. Assuming each peak can be assigned entirely to a single site, D/a^2 can be calculated as a function of T and the activation energy determined. Activation energies for the three sites appear to be roughly 30, 60, and 90 kcal/mol, with the ^{39}Ar equally distributed among the sites (A. R. Gillespie et al., manuscript in preparation, 1982). From Figure 7 it is clear that this range in Q is sufficient to yield an eruption age plateau extending over at least a third of the spectrum. Indeed the age spectrum in Figure 8 resembles that of a model xenolith with multiple diffusion sites of sufficiently different diffusivities as to separate the Ar from nonretentive phases and residual ^{40}Ar from other more retentive phases during extraction in the laboratory. Of the theoretical spectra shown in Figure 6, the one for model 'e' (spheres of the same size but two activation energies: 30 and 75 kcal/mol) most closely resembled the age spectrum found for the real xenolith (note that the ordinate in Figure 6 is logarithmic). Thus it appears that diffusion of Ar from the quartz monzonite xenolith can be reasonably well described by volume diffusion from grains having different diffusivities but not from identical grains, and the theoretical considerations presented in this paper have some justification in terms of the behavior of actual systems.

4. CONCLUSIONS

It appears possible under some conditions to determine the age of eruption of a lava from plateaus in the ^{40}Ar-^{39}Ar age spectra of xenoliths which were only partially degassed during incorporation in the magma and eruption. The factors affecting the development of a plateau at the age of degassing or eruption are (1) the extent of degassing of the xenolith in the host magma, (2) the original crystallization age of the xenolith relative to the time of degassing by the host magma, (3) the distribution in grain size or $a/\sqrt{D_0}$ of the contributing minerals in the xenolith, and (4) the activation energies for Ar diffusion from the minerals in the xenolith. For such a plateau to exist there must have existed ^{40}Ar reservoirs which could be completely degassed by the magma, and during laboratory analysis no other reservoir released residual ^{40}Ar in quantities large enough to increase significantly the apparent age during release of Ar from those nonretentive reservoirs. The factors which determine whether or not this is possible are interdependent, but the basic necessary conditions seem to be degassing in the magma of more than ~90% of the Ar and the presence of multiple sites for Ar characterized by different values of D_0, a, or Q. For the

bimodal models considered in detail here, values of grain size must differ by more than an order of magnitude or values of Q must differ by more than ~12 kcal/mol if one activation energy is 30 kcal/mol. If these conditions are satisfied, it should prove possible to identify the age of eruption of Pleistocene lavas even if the age of original crystallization of the xenolith was 2 orders of magnitude greater. These conditions must be exceeded if incorporated xenoliths are substantially older or the lavas to be dated are substantially younger. The extensive low-temperature plateau at 1.2 m.y. in the age spectrum of a partially degassed granitic xenolith from a Pleistocene basalt flow confirms the basic conclusions of this analysis.

Acknowledgments. This research was supported by NSF grants EAR 78-01787 and EAR 79-19997. F. Begemann improved the presentation through his detailed criticisms and suggestions. The presentation also benefitted from the reviews of G. Turner and two anonymous reviewers. Contribution 3649 (399) of the Division of Geological and Planetary Sciences, California Institute of Technology.

REFERENCES

Baadsgaard, H., J. Lipson, and R. E. Folinsbee, The leakage of radiogenic argon from sanidine, *Geochim. Cosmochim. Acta, 25,* 147–157, 1961.

Berger, G. W., ^{40}Ar-^{39}Ar step heating of thermally overprinted biotites, hornblendes, and potassium feldspars from Eldora, Colorado, *Earth Planet. Sci. Lett., 26,* 387–408, 1975.

Carslaw, H. S., and J. C. Jaeger, *Conduction of Heat in Solids,* p. 233 (510 pp.), Clarendon, Oxford, 1959.

Crank, J., *The Mathematics of Diffusion,* 347 pp., Clarendon, Oxford, 1956.

Dalrymple, G. B., Argon retention in a granitic xenolith from a Pleistocene basalt, Sierra Nevada, California, *Nature, 201,* 282, 1964.

Dalrymple, G. B., and M. A. Lanphere, $^{40}Ar/^{39}Ar$ technique of K-Ar dating: A comparison with the conventional technique, *Earth Planet. Sci. Lett., 12,* 300–308, 1971.

Evernden, J. F., G. H. Curtis, R. W. Kistler, and J. Obradovich, Argon diffusion in glauconite, microcline, sanidine, leucite, and phlogopite, *Am. J. Sci., 258B,* 583–604, 1960.

Fechtig, F., W. Gentner, and J. Zähringer, Argonbestimmungen an Kaliummineralien, VII, Diffusionsverluste von Argon in Mineralien und ihre Auswirkung auf die Kalium-Argon-Alterbestimmung, *Geochim. Cosmochim. Acta, 19,* 70–79, 1960.

Foland, K. A., Ar^{40} diffusion in homogeneous orthoclase and an interpretation of Ar diffusion in K-feldspars, *Geochim. Cosmochim. Acta, 38,* 151–166, 1974.

Gillespie, A. R., Quaternary glaciation and tectonism in the southeastern Sierra Nevada, Inyo County, California, Ph.D. thesis, 695 pp., Calif. Inst. of Tech., Pasadena, 1982.

Hart, S. R., The petrology and isotopic-mineral age relations of a contact zone in the Front Range, Colorado, *J. Geol., 72,* 493–525, 1964.

Jäger, E., E. E. Niggli, and H. Baethge, Two standard minerals, biotite and muscovite, for Rb-Sr and K-Ar age determinations, sample Bern 4B and Bern 4M from a gneiss from Brione, Valle Verzasca (Switzerland), *Schweiz. Mineral. Petrogr. Mitt., 43,* 465–470, 1963.

Moore, J. G., Geology of the Mount Pinchot quadrangle, southern Sierra Nevada, California, *U.S. Geol. Surv. Bull., 1130,* 152 pp., 1963.

Radicati di Brozolo, F., J. C. Huneke, D. A. Papanastassiou, and G. J. Wasserburg, ^{40}Ar-^{39}Ar and Rb-Sr age determinations on Quaternary volcanic rocks, *Earth Planet. Sci. Lett., 53,* 445–456, 1981.

Reichenberg, D., Properties of ion-exchange resins in relation to their structure, III, Kinetics of exchange, *J. Am. Chem. Soc., 75,* 589–597, 1953.

Steiger, R. H., and E. Jäger, Subcommission on geochronology: Convention on the use of decay constants in geo- and cosmochronology, *Earth Planet. Sci. Lett., 36,* 359–362, 1977.

Turner, G., The distribution of K and Ar in chondrites, in *Origin and Distribution of the Elements,* edited by L. H. Ahrens, pp. 387–398, Pergammon, New York, 1968.

(Received April 14, 1982;
revised July 12, 1982;
accepted July 28, 1982.)